

Estimation of Obstacle and Terrain Impact Probabilities

Robert S. Swanson* and Samuel A. Musa†
Institute for Defense Analyses, Arlington, Va.

This paper presents some new methods for estimating the probability of impact of a terrain-following cruise missile into obstacles, terrain anomalies, and bald terrain. Estimates of the impact probability are determined for a missile penetrating an area with randomly located obstacles and the effects of navigational-reconnaissance errors on the impact probabilities are investigated. The bold terrain impact probability of a missile with a linear altitude control system having either a downward or a forward looking sensor is determined with emphasis on terrain whose power spectral density decays at 20 dB/decade for which previously published methods could not be used.

Introduction

THE realistic estimation of terrain- and obstacle-impact probabilities is a very difficult problem. Methods of estimating the probability of impact for flight over bald terrain have been extensively studied for about two decades.¹⁻³ On the other hand, methods of estimating the probability of impacting obstacles have not been discussed in the literature except in the sense of recommending some minimum value of the flight altitude to allow a margin to avoid such obstacles. During the study treated here it became apparent that for many regions of interest the probability of impacting obstacles for very low-altitude flight (less than 60 m) exceeds the probability of impacting relatively flat bald terrain. Methods of analyzing the obstacle problem were therefore developed and are discussed in the following section.

Also presented are analytic estimates of the probability of impact for cruise missiles traversing bald terrain using either an altimeter or a forward-looking sensor. Analytic estimates had been previously given for linearized terrain-following altimeter-only controlled cruise missiles for the cases where the terrain characteristics in terms of power spectral density are such that the power spectral density decreases at a rate of 40 dB/dec or greater. The analytic techniques previously used were not suitable for terrain whose power spectral density decreases at 20 dB/dec.

Obstacle and Terrain Anomaly Impact Probability Estimates for Downward-Looking Sensor Systems

Generally, analyses of downward-looking control systems indicate small probabilities of impact of cruise missiles for low-altitude flight over bald terrain. Unfortunately, there are a large number of natural and man-made obstacles as well as terrain anomalies which, if not accounted for, considerably increase the probability of impact for downward-looking systems. Typical obstacles which must be considered are power lines, church steeples, smokestacks, windmills, vegetation (including forests, stand-alone tall trees, tree-lined highways, etc.), and tall buildings. In addition to these obstacles, it is convenient to group certain classes of "terrain anomalies" with the obstacles, since the impact probability estimation procedures are similar for the two cases. Unfortunately, a terrain-anomaly must be defined as a piece of terrain which, if the missile attempts to overfly at a particular altitude and speed and with particular control characteristics, it will impact the terrain. Thus, the impact probability depends not only on the characteristics of the terrain anomaly itself, but also on the flight characteristics of the missile. The

concept of "design profiles" is proposed as a way of analyzing the terrain anomaly problem. The design profiles are idealized models of terrain anomalies for which some specific characteristics of the profile for the particular command altitude, vehicle speed, and control system gain settings. Under these conditions the specified ramp or any ramp with steeper slopes becomes a "terrain anomaly." The grouping of terrain anomalies and obstacles together allows a more straight-forward appreciation of the accuracy of linearized terrain following altimeter-only controlled cruise missile probability predictions over bald terrain; i.e., these estimates require that we be able to characterize the terrain amplitude distribution as gaussian, and if it deviates from the gaussian distribution we may characterize that deviation as contributing to "terrain anomalies." Note that a terrain anomaly, therefore, can be a critical terrain profile which occurs between two individually homogeneous terrain populations; each of these may have gaussian amplitude distributions and a critical terrain profile occurring in a uniform population of terrain which has a non-gaussian distribution superimposed on a gaussian amplitude distribution.

There are two general procedures for avoiding obstacles. The first is to use a forward-looking sensor to detect the obstacle and to use a missile-borne computer to command the control system to avoid the obstacle, by either going around it or over it. (This is the way almost all aircraft terrain-following systems are employed.) The second case proposed for cruise missiles involves using a downward-looking sensor system and preplanning the flight path to avoid all known obstacles. If the navigational and reconnaissance errors are small, a downward-looking terrain system will be satisfactory. The downward-looking terrain following system does involve 1) very extensive and expensive reconnaissance data, and 2) keeping a complete catalog of obstacle positions and characteristics in the computer memory of the cruise missile. The second case is analyzed below.

Let us consider a rectangular area containing randomly located obstacles. The axis of this rectangular area will be parallel and perpendicular to the general average flight path direction, the distance along the flight path being designated the X direction and across the flight path the Y direction. In general, the density of the obstacles will not be constant, that is, the mean distance between obstacles will be different in the two orthogonal directions, along the flight path and at right angles to the flight path. The mean distance between obstacles along the flight path will be designated S_X (km) and the mean distance between obstacles in a direction at right angles to the flight path is S_Y (km). If the density of obstacles is equal in both directions then $S_X = S_Y = S = 1/\sqrt{\rho}$ (km), where ρ is the average density of obstacles (per km²). On the average, R/S_X obstacles will be potentially encountered in traversing a distance R (range in km).

It is probably easiest to visualize the case where $S_X \neq S_Y$ for a general area over which the cruise missile will traverse,

Presented as Paper 75-1118 at the AIAA Guidance and Control Conference, Boston, Mass., Aug. 20-22, 1975; submitted Aug. 27, 1975; revision received March 4, 1976.

Index categories: LV/M Guidance Systems, LV/M Mission Studies and Economics.

*Member of Professional Staff. Associate Fellow AIAA.

†Member of Professional Staff.

which is composed of many equal-sized rectangles, each of which (on the average) contains one obstacle and whose dimensions are S_X in the direction of the flight path and S_Y in the direction perpendicular to the flight path. Of course, in actuality, these dimensions are the mean distances between obstacles. Some rectangles will contain no obstacles and others will contain two or more obstacles, but, on the average, each rectangle $S_X S_Y$ will contain a single obstacle somewhere within the rectangle.

The probability of encountering an obstacle in passing through the first series of rectangles $P_{[(R/S_X)=1]}$ (i.e., traversing the first mean distance between obstacles, S_X) is calculated assuming there is, on the average, a single obstacle in rectangle $S_X S_Y$. The probability is equal to

$$P = \gamma D / S_Y \quad (1)$$

where D is the effective encounter diameter of a cruise-missile/obstacle combination (cruise missile wing span plus obstacle lateral dimensions in kms). The term γ is the clearance histogram factor and is numerically equal to the fraction of the distance along the flight path for which the vehicle altitude is less than the altitude of the top of the obstacle being considered. Estimating γ involves the effective use of histograms of the clearance altitudes for each particular situation considered. A feel for the numerical magnitude of γ can be derived from the following case, estimated for smooth terrain with a detrended standard deviation, $\sigma_T = 30$ m and a cruise missile terrain-following control system with a control bandwidth of about 1 rad/sec so $(\sigma_e/\sigma_T) = 0.2$ and $\sigma_e = 6$ m, where σ_e is the standard deviation of the terrain-following control system errors. For a randomly placed obstacle 30 m high, a cruise missile with mean altitude of 30 m will hit the obstacle one-half the time if its flight path is straight toward the obstacle. If the mean flight altitude is 30 m, the cruise missile will go over the top of the obstacle 25% of the time ($\gamma = 0.75$) if the obstacle is 34 m ($0.67 \sigma_e = 4$ m) high. The missile will go over the top of the obstacle 75% of the time ($\gamma = 0.25$) if the obstacle is 26 m high. Note that γ changes rapidly with obstacle altitude and again for the mean flight altitude of 30 m if the obstacle is over 40 m ($1.64 \sigma_e = 9.8$ m) high $\gamma \geq 0.95$, and if the obstacle is less than 20 m high, $\gamma \leq 0.05$. Note that the standard deviation of the error is directly proportional to the standard deviation of the terrain. Thus, γ will change twice as fast with flight altitude if the terrain standard deviation is only 15 m than it will for the previous example for a 30 m terrain standard deviation.

If one traverses along the flight path a distance R , then, on the average, one will encounter R/S_X independent regions, each containing an obstacle. Strictly speaking, R/S_X should be evaluated at the closest integer value. It makes little difference, however, for large values of R/S_X . The probability of impact during this traverse is

$$P = 1 - [1 - (\gamma D / S_Y)]^{R/S_X} \quad (2)$$

Figure 1 gives the probability of impact as a function of $\alpha \gamma D R / S_Y S_X$ for a range of values of the mean number of obstacles traversed R/S_X . The navigational-reconnaissance factor α will be defined in the following, and is equal to 1 for the random obstacle location case of Eqs. (1) and (2).

So far, we have estimated the probability of impacting obstacles if the obstacles were randomly located. We can extend this basic method to include the case where we have determined the position of the obstacles from reconnaissance data and have preprogrammed the cruise missile to go between pairs of obstacles. Since the navigational system, as well as the reconnaissance data, contains errors, it will be quite possible for the missile to run into one of the obstacles. The discussion is limited to the downward-looking terrain-following system, since a properly designed forward-looking system could avoid the possibility of impact because it can "see" the obstacles and then maneuver to avoid them.

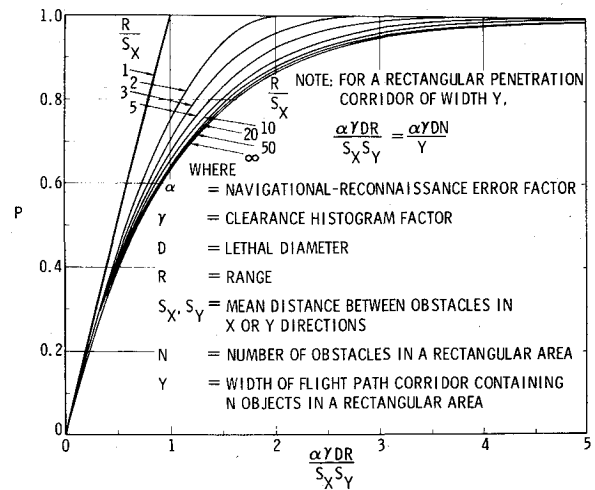


Fig. 1 Probability of impacting randomly located obstacles as a function of the parameter, $\alpha \gamma D R / S_Y S_X$.

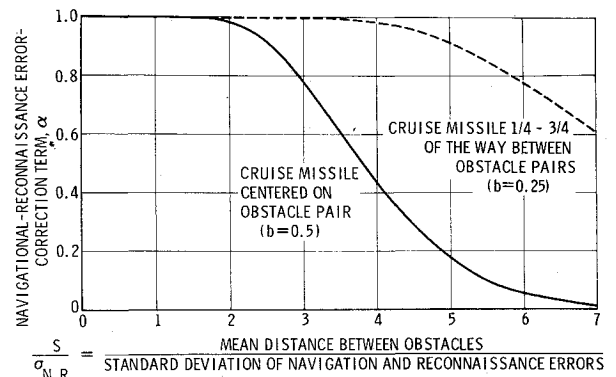


Fig. 2 Navigational-Reconnaissance error factor α .

The equation for determining the impact probability, including the influence of navigational and reconnaissance errors on a preprogrammed downward-looker can be arranged in the same format as the random case [Eq. (2)]. A parameter α , whose numerical value lies between zero and unity, can be used to multiply the lethal encounter diameter to obtain an "effective" lethal encounter diameter. The parameter α is a function of the distance between the obstacles and the standard deviation of the reconnaissance and navigational errors $\sigma_{N,R}$, where $\sigma_{N,R} = (\sigma_N^2 + \sigma_R^2)^{1/2}$ and σ_N is the standard deviation of the navigational errors, km, and σ_R is the standard deviation of reconnaissance errors, km. That is, Eq. 2 becomes

$$P = 1 - \left(1 - \frac{\alpha \gamma D}{S_Y}\right)^{R/S_X} \quad (3)$$

The reconnaissance and navigational error factor α can be estimated by assuming the navigational errors to be normally distributed about the desired lateral location of the flight path and the reconnaissance errors to be normally distributed about the location of the obstacles. For purposes of analysis, the obstacles are assumed to be exactly equally spaced. In actual practice, of course, they will be randomly spaced with a mean distance between obstacles equal to S_Y . For a general flight path position located a fraction b between $(N/2)$ obstacle pairs, α can be determined as

$$\alpha = \frac{S_Y}{\sqrt{2\pi}\sigma_{N,R}} \sum_{n=1}^{N/2} \left[\exp\left(-\frac{(n-1+b)^2 S_Y^2}{2\sigma_{N,R}^2}\right) + \exp\left(-\frac{(n-b)^2 S_Y^2}{2\sigma_{N,R}^2}\right) \right] \quad (4)$$

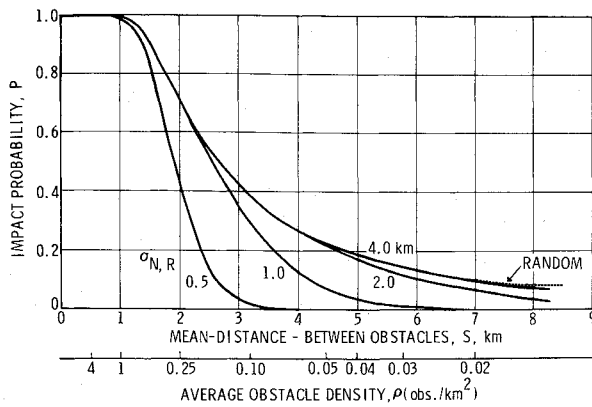


Fig. 3 Probability of impacting obstacles for preprogrammed downward-looking terrain-following system, $D = 5$ m, $R = 1000$ km, $\gamma = 1.0$; centered on obstacle pairs.

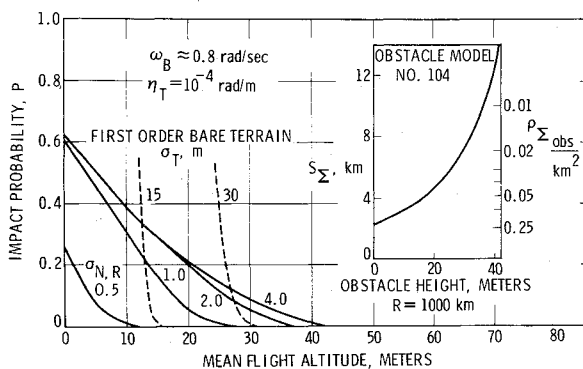


Fig. 4 Impact probabilities altimeter-only controls, bare terrain and obstacle model no. 104.

Numerical values of α are given in Fig. 2 for two cases, 1) where the vehicle is preprogrammed to go exactly halfway between an obstacle pair ($b=0.5$), and 2) where the cruise missile is preprogrammed to go one-quarter of the way between the obstacle pair ($b=0.25$), a case where one attempts to decrease the flight path deviations required to go halfway between obstacles. Note that it is clearly desirable to go halfway between obstacles when at all possible unless the mean distance between these obstacles is very great.

If the locations of all obstacles are known with high precision relative to the mean distance between obstacles S , the parameter $(S/\sigma_{N,R})$ is larger and α is small, and thus the probability of hitting the obstacles is small. To make realistic estimates of the probability of impacting obstacles, it is necessary to have statistical data on the mean distance between obstacles of different heights and to estimate numerical values of $\sigma_{N,R}$.

Using these equations, we can estimate the obstacle-impact probabilities for several representative cases. Because, in most instances, accurate obstacle statistics and accurate estimation of σ_N and σ_R are not available, the data in the following paragraphs will be primarily presented in parametric form.

Figure 3 gives the obstacle-impact probability as a function of the mean distance between obstacles and of the standard deviation of the navigational and reconnaissance errors, for the case where the vehicle is flying well below the height of the obstacles, i.e., $\gamma=1$. The envelope of the upper curves is the case where $\alpha=1$, i.e., the navigational errors are sufficiently large relative to the mean distance between obstacles that it makes no difference whether we attempt to go between obstacles, or simply assume the obstacles are randomly located and make no attempt to avoid them. Over the reasonable range of the mean distance between obstacles, and of the standard deviation of the navigational and reconnaissance errors, it can be seen there is a significant probability of impacting obstacles in a 1000 km flight.

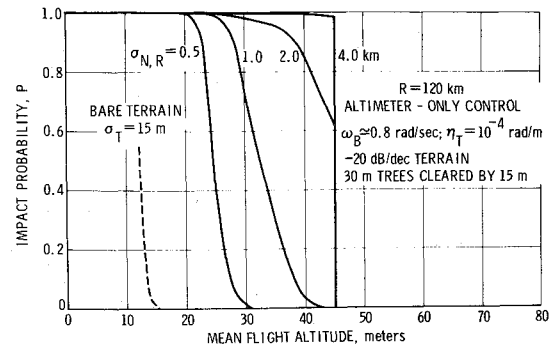


Fig. 5 Two-dimensional obstacle (tree-lined highways for a 120^2 km^2 region, $S = 8$ km).

In order to account for the actual height of the obstacles, it is necessary to assume some variation of obstacle height and of the mean distance between obstacles. It is clear that there are very few, very tall obstacles, but a great many short obstacles. Although there is little actual data from which one can make an estimate of the relation between obstacle height H_{obs} and mean distance between obstacles of a height greater than H_{obs} , one reasonable variation is shown in the inset diagram of Fig. 4. It is believed that if this model errs in any way, it is probably overly conservative in specifying too few high obstacles. Using the variation of obstacle height and mean distance between obstacles, one can evaluate the terrain-following control system histogram for specific configurations and thus determine the impact probabilities as a function of the mean altitude which it is desired to fly for a given range. For comparison purposes, the impact probabilities associated with bare terrain are included in this figure. The parameter ω_B given on Fig. 4 is the control system bandwidth, rad/sec, and η_T is the spatial bandwidth frequency (the frequency where the power spectral density is 3 dB down from the asymptotic value at zero frequency) rad/m. Actual numerical procedures for calculating the bald terrain impact probabilities will be discussed in the next section. For flight at very low altitudes, the probabilities of impacting obstacles exceeds the probability of impacting bald terrain, especially if the average σ_T over the 1000 km of low altitude is about 15 m and $\sigma_{N,R}$ is greater than 1 km.

So far, we have discussed one-dimensional (stand-alone) obstacles and terrain anomalies. A different type of analysis is required for two-dimensional obstacles and terrain anomalies. Two-dimensional obstacles are defined as those obstacles too wide for the cruise missile flight path to conveniently be rerouted to go around, thus it is necessary to go over them. Two-dimensional obstacles are typically power lines, tree-lined highways, the edge of forests, cliffs, mountain ridges, and man-made barriers such as steel cables hung between trees, towers, or barrage balloons.

As an illustrative example of the two-dimensional obstacle problem, let us assume that tree-lined highways have a mean spacing of about 8 km for a particular region, 120^2 km^2 . The trees have an average height of 30 m. The impact probability as a function of mean flight altitude and standard deviation of the navigational and reconnaissance errors is given in Fig. 5. The dotted curves are the terrain-impact probabilities which will be estimated in the next section. If the standard deviation of the navigational and reconnaissance errors is more than a couple of kilometers, then it will be necessary to fly at a mean flight altitude of at least 45 m for the 120^2 km^2 area. The desirability of having a forward-looking sensor is evident.

Bald Terrain Impact Probability Estimates

This section provides an analytic estimate of the probability of impact of a terrain-following cruise missile with a linear altitude control system having either a downward-looking (altimeter) or a forward looking sensor. The forward-looking

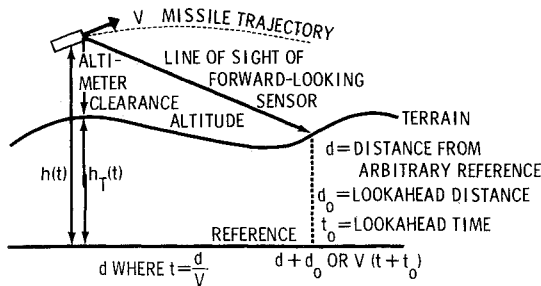


Fig. 6 Linearized altitude control system block diagram (altimeter-only).

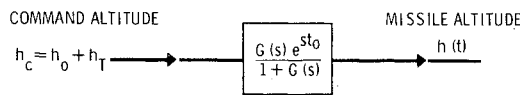


Fig. 7 Linearized altitude control system (forward-looking).

sensor enhances the terrain-following capability, since it provides more anticipation of the terrain to be overflown; however, such a sensor increases the chance of enemy detection of the terrain-following missile.

The probability of impact of a missile equipped with a second-order control system flying over a terrain whose power spectral density is of the Butterworth form is investigated, with special emphasis on the first-order terrain (φ decreases at 20 dB/dec). The analytic model of the downward-looking control system is believed to give quite realistic results. The model for the forward-looker is more approximate, but should give a conservative estimate of the degree of lower-altitude flight over bald terrain that is possible with forward-lookers. Of course, the main advantage of forward-lookers is that they provide a capability for obstacle avoidance, as discussed in the body of this paper. The limitations of the analytic model for the terrain-following control system with the forward-looking sensor are carefully discussed.

The probability of impact of a terrain-following cruise missile can be evaluated analytically, given a statistical model of the terrain and a linearized version of a missile's altitude control system. The linearized altitude control loop is shown in Fig. 6, where: 1) $h(t)$ is the altitude (as a function of time, t) of the missile above a fixed reference; 2) $h_T(t)$ is the altitude of the terrain above the same reference; 3) h_0 is the command value of the constant clearance altitude; and 4) $e(t) = h_0 - [h(t) - h_T(t)] = h_0 + h_T(t) - h(t)$ is the altitude error. The linear look-ahead case can be treated by considering the control system for which the driving terrain is just the real terrain displaced by the look-ahead time (Fig. 7). The primary limitation of this model of the linear look-ahead case is that it assumes the sensor can "look through" any intervening terrain.

The impact probability can be calculated from the zero-crossing theory for random gaussian processes^{4,5}. In particular, we have to evaluate the probability that the altitude error $e(t)$ crosses the command clearance altitude h_0 [$h(t) = h_T(t)$ so that $e(t) = h_0$] with the error slope $e'(t) > 0$ for a given flight path of duration T sec. The probability that $e(t)$ crosses h_0 with $e'(t) > 0$ in the time interval $(t, t + \tau)$, where τ is small, is given⁵ by

$$p(\tau) = \frac{1}{2\pi} \left\{ \frac{2[R_e(0) - R_e(\tau)]}{R_e(0)} \right\}^{1/2} e^{-h_0^2/2R_e(0)} \quad (5)$$

where $R_e(\tau)$ is the autocorrelation function of the altitude error, and $R_e(0)$ is the variance of the altitude error (σ_e^2). For small τ , $R_e(\tau)$ can be approximated by

$$R_e(\tau) = R_e(0) + R_e'(0)\tau + \frac{R_e''(0)\tau^2}{2} + \dots \quad (6)$$

Since $R_e(\tau)$ is even, then its derivative, if it exists, must be equal to zero at the origin. Hence Eq. (5) reduces to

$$p(\tau) = \lambda\tau, \lambda = \frac{1}{2\pi} \left[-\frac{R_e''(0)}{R_e(0)} \right]^{1/2} e^{-h_0^2/2R_e(0)} \quad (7)$$

where λ is the number of zero crossings per second. Since $-R_e''(0)$ is the variance of the altitude error rate $\sigma_e'^2$, the terms in the brackets in expression (7) reduce to (σ_e'/σ_e) and the well-known expression for λ is obtained. Assuming that the events of ground impact in a time interval T are Poisson-distributed with mean frequency λ , then the probability of n impacts in T sec is $[(\lambda T)^n/n!] \exp(-\lambda T)$. The probability of not hitting the ground in T sec is then $\exp(-\lambda T)$. Therefore, the probability of impact (one or more impacts in T sec) is

$$P = 1 - \exp \left[-\frac{T}{2\pi} \frac{\sigma_e'}{\sigma_e} \exp \left(-\frac{h_0^2}{2\sigma_e^2} \right) \right] \quad (8)$$

This relationship can be used to evaluate the impact probability from simulation data on $(h_0, \sigma_e, \sigma_e', T)$, assuming the altitude error process is ergodic and both altitude error and error rate are normally distributed.

Detailed investigations of the probability of impact were made in Ref. 3 for terrains with power spectral densities of the Butterworth form:

$$\varphi(\eta) = \frac{K_n \sigma_T^2 / \eta_T}{1 + (\eta / \eta_T)^{2n}} \quad (9)$$

where η_T is the terrain-break frequency (rad/m). However, the probability of impacting a first-order terrain ($n=1$) could not be evaluated in Ref. 3 because the expression for $\sigma_e'^2$ diverges. The expression for $\sigma_e'^2$ can be made to converge by approximating the power spectral density of a first-order terrain with that of a higher-order terrain.

$$\varphi(\eta) = \frac{2\sigma_T^2 / \eta_T}{1 + (\eta / \eta_T)^2} \approx \frac{2(1+2\epsilon)^{1/2} (\sigma_T^2 / \eta_T)}{1 + (\eta / \eta_T)^2 + \epsilon^2 (\eta / \eta_T)^4} \quad (10)$$

Although the approximation to the first-order terrain by Eq. (10) with $\epsilon = 10^{-4}$ appears to be reasonable, a computation of the probability of impact as a function of ϵ shows better agreement is obtained, assuming a value of $\epsilon = 10^{-2}$. It should be emphasized that it is difficult to assess the accuracy of the probability of impact via the approximation [Eq. (10)] without the results of the direct method to be presented below. One would resort to such an approximation only if one did not realize that a direct estimate was possible.

A more direct method for computing the probability of impact for a first-order terrain is to use the singular case of the zero-crossing theory.⁵ In the singular case, where the derivative $R_e'(\tau)$ is discontinuous at $\tau=0$, Eq. (6) becomes $R_e(0) + R_e'(0^+)\tau$. The second-order terms in τ are neglected and $R_e'(0^+)$ is the right-side derivative of $R_e(\tau)$. Thus, Eq. (5) reduces to

$$p_I(\tau) = \frac{1}{2\pi} \left[-\frac{2R_e'(0^+)\tau}{R_e(0)} \right]^{1/2} e^{-h_0^2/2R_e(0)} \quad (11)$$

If we let $\tau = \tau_I^2$, then $p_I = \lambda_I \tau_I$, where

$$\lambda_I = \frac{1}{2\pi} \left[-\frac{2R_e'(0^+)}{R_e(0)} \right]^{1/2} \exp[-h_0^2/2R_e(0)]$$

Again, assuming the events of ground impact in time interval \sqrt{T} to be Poisson-distributed, with mean frequency λ_I , the probability of impact becomes

$$P = 1 - \exp \left[-\frac{1}{2\pi} \left\{ -\frac{2R'_e(0^+)T}{R_e(0)} \right\}^{\frac{1}{2}} e^{-h_0^2/2R_e(0)} \right] \quad (12)$$

where $R_e(0) = \sigma_e^2$ and $R'_e(0^+)$ is the right-side derivative of the autocorrelation function of the altitude error.

Now let us compute the probability of impact for a first-order terrain as expressed by the power spectral density (Eq. 9) with $n=1$, $K_n=2$. The autocorrelation function of the altitude error is given by

$$R_e(\tau) = \frac{1}{2\pi} \int_{-\infty}^{\infty} \varphi_e(\omega) e^{i\omega\tau} d\omega \quad (13)$$

where $\varphi_e(\omega)$ is the power spectral density of the altitude error. Note that $\omega = \eta V$ rad/sec, where V is the missile velocity. Since the power spectral density of the output of a linear system with a transfer function $A(\omega)$ is given by the product of $|A(\omega)|^2$ and the power spectrum of the input, the power spectral density of the altitude error $\varphi_e(\omega) = |H_e(\omega)|^2 \varphi(\omega)$. $H_e(\omega)$ denotes the transfer function from command altitude $[h_0 + h_T(t)]$ to altitude error. Note that $H_e(\omega) = 1 - H(\omega)$, where $H(\omega) = G(\omega)/[1 + G(\omega)]$ is the closed-loop transfer function of the control system in Fig. 6. The autocorrelation function of the altitude error $R_e(\tau)$ for a second-order control system with transfer function

$$H(s) = \frac{1}{(s/\omega_B) + \sqrt{2}(s/\omega_B) + 1}$$

is evaluated by using Eq. (13) to yield

$$\begin{aligned} \frac{R_e(\tau)}{\sigma_T^2} &= \frac{\sqrt{5\theta}}{(1+\theta^4)^{\frac{1}{2}}} e^{-\omega_B |\tau| / \sqrt{2}} \cos \left(\frac{\omega_B |\tau|}{\sqrt{2}} - \Psi \right) \\ &+ \frac{(1-2\theta^2)}{1+\theta^4} e^{-\omega_T |\tau|} \end{aligned} \quad (14)$$

where $\theta = (\omega_B/\omega_T)$, and $\Psi = \tan^{-1} \left(\frac{\theta^2 - 3}{1 + 3\theta^2} \right)$.

The derivative of $R_e(\tau)$ as expressed in Eq. (14) is discontinuous at $\tau=0$. The right-side derivative $R'_e(0^+)$ is equal to $-\omega_T$. Thus, Eq. (12) becomes

$$P = 1 - \exp \left[-\frac{1}{2\pi} \left\{ 2\omega_T T \left(\frac{\theta^2 + \sqrt{2\theta} + 1}{3\theta/\sqrt{2} + 1} \right) \right\}^{\frac{1}{2}} Z \right] \quad (15)$$

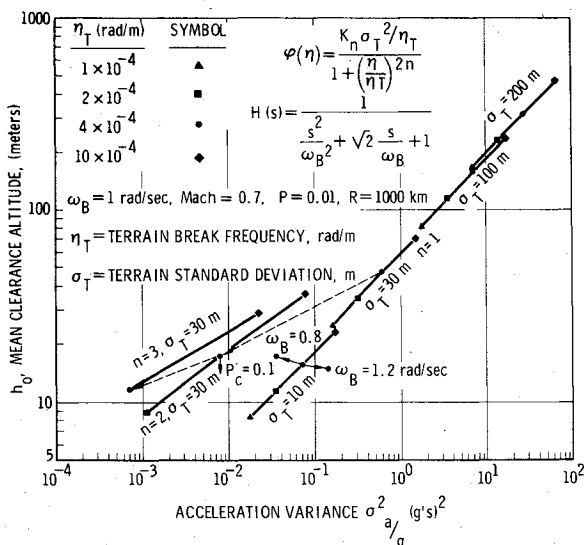


Fig. 8 Effect of terrain characteristics.

where

$$Z = \exp \left(-\frac{h_0^2 (\theta^2 + \sqrt{2\theta} + 1)}{2\sigma_T^2 (3\theta/\sqrt{2} + 1)} \right)$$

which is the probability of impact of a terrain-following missile with a second-order control system flying over a first-order terrain. To examine the relationship between the command altitude clearance h_0 and the missile normal acceleration, the expression for the variance of the normal acceleration has to be computed. The power spectral density of the normal acceleration is given by $|H_a(\omega)|^2 \varphi(\omega)$, where $H_a(\omega) = -\omega^2 H(\omega)$. Clearly then,

$$\sigma_a^2 = \frac{1}{2\pi} \int_{-\infty}^{\infty} |H_a(\omega)|^2 \varphi(\omega) d\omega \quad (16)$$

is the variance of the normal acceleration. For a first-order terrain and a second-order control system, Eq. (16) reduces to

$$\frac{\sigma_a^2}{\omega_T^4 \sigma_T^2} = \frac{\theta^4 (1 + 0.5\sqrt{2\theta})}{1 + \sqrt{2\theta} + \theta^2} \quad (17)$$

which is the normalized variance of normal acceleration.

The relationship between the command altitude and the normal acceleration variance is evaluated from Eqs. (15) and (17), and is shown in Figs. 8 and 9. Figure 8 gives the dimensional characteristics of the mean clearance altitude and acceleration variance for several different terrains while Fig. 9 gives the normalized command altitude and acceleration variance for first-order terrain. In Fig. 8 the control frequency bandwidth is fixed at $\omega_B = 1$ rad/sec, while the terrain-break frequency η_T is varied from 10^{-4} to 10^{-3} rad/m. The higher the terrain-break frequency, the greater the command clearance altitude (since the mean of altitude error is zero, the mean clearance altitude is equal to command clearance altitude h_0) necessary to achieve a fixed level of probability of impact ($P=0.01$ for a range of 1000 km or $P=0.001$ for a range of 100 km). As expected (Fig. 9), the rougher the terrain (greater standard deviation σ_T), the higher the command clearance altitude. The command clearance altitude and normal acceleration for a second- and third-order terrain are derived and shown in Fig. 8 for $\sigma_T = 30$ m.

The result is that the increase in command clearance altitude and normal acceleration with decreasing order terrain is quite significant. The effect of increasing the probability of impact on the command altitude is shown by an arrow in Fig. 8. As expected, the lower the command clearance altitude, the higher the probability of impact.

The varying parameters in Fig. 9 are the control system break frequency and missile velocity. The acceleration variance increases with increasing bandwidth of the terrain-following control system, terrain standard deviation, and missile velocity. By increasing the control bandwidth, it is

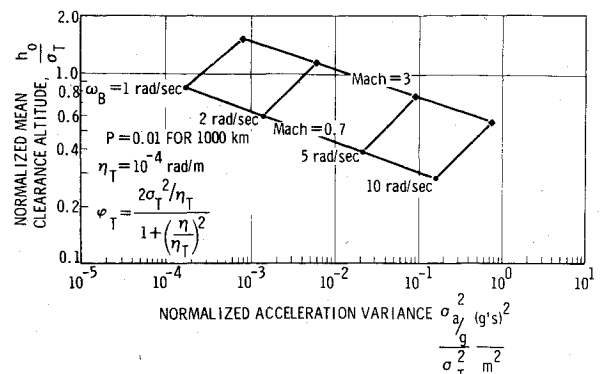


Fig. 9 Effects of speed and control system bandwidth parameter, ω_B (first-order terrain).

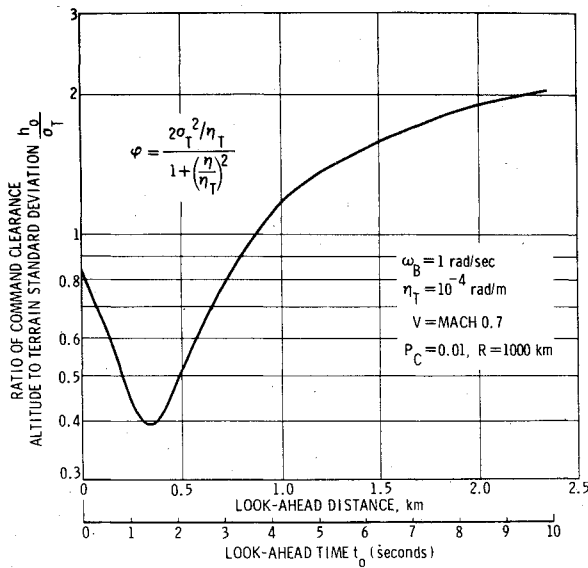


Fig. 10 Effect of forward-looking system on command altitude.

possible to reduce the command altitude, but with a considerable increase in acceleration variance and resulting range loss. Furthermore, the command altitude increases with increasing missile velocity and associated increase in acceleration variance.

The probability of impact of a terrain-following missile with a forward-looking sensor can be approximated by using the analysis of the previous sections and by driving the control system with the real terrain displaced by the look-ahead time. In this case, the closed-loop transfer function of the control system becomes $H(s)e^{st_0}$, where t_0 is the look-ahead time (Fig. 7). The autocorrelation function of the altitude error [Eq. (13)] becomes, in this case

$$R_e(\tau) = \frac{1}{2\pi} \int_{-\infty}^{\infty} H_0(\omega) H_0(-\omega) \phi(\omega) e^{i\omega\tau} d\omega \quad (18)$$

where $H_0(\omega) = 1 - H(\omega)e^{i\omega t_0}$. Expression (18) was evaluated for a first-order terrain [Eq. (9) with $n=1$] and the second-order control system, and the normalized variance of the altitude error becomes

$$\frac{\sigma_e^2}{\sigma_T^2} = \frac{1 + 1.5\sqrt{2\theta} + 2\theta^2}{1 + \sqrt{2\theta} + \theta^2} - \frac{2\theta^2 e^{-\omega_T t_0}}{1 - \sqrt{2\theta} + \theta^2} + \frac{4\sqrt{2\theta} e^{-\omega_B t_0/\sqrt{2}}}{(1 + \theta^4)^{1/2}} \cos\left(\frac{\omega_B}{\sqrt{2}} t_0 + \Psi\right) \quad (19)$$

The derivative of $R_e(\tau)$ is discontinuous at $\tau=0$, with a right-hand side value of $R'_e(0^+) = -\omega_T$. Thus, the probability of impact as expressed by Eq. (12) becomes

$$P = 1 - \exp\left[-\frac{1}{2\pi} \left(\frac{2\omega_T T}{\sigma_e^2/\sigma_T^2}\right)^{1/2} \exp\left(-\frac{h_0^2/\sigma_T^2}{\sigma_e^2/\sigma_T^2}\right)\right] \quad (20)$$

where σ_e^2/σ_T^2 is given by Eq. (19). Equation 20 represents the probability of impact of a terrain-following missile with a forward-looking sensor and a second-order control system flying over a first-order terrain. The variance of the normal acceleration for the forward-looking sensor is the same as the downward-looking altimeter as expressed by Eq. (17), because the model of the linear look-ahead case assumes the missile is flying over the look-ahead terrain.

The improvement in the terrain-following capability with a forward-looking sensor is demonstrated in Fig. 10. As the look-ahead time increases to 1.5 sec (at Mach=0.7, 1.5 sec

corresponds to 357 m), the command clearance altitude can be reduced by a factor of one-half in comparison with the downward-looking case ($t_0=0$) for the same probability of impact.

The reason that the command clearance altitude increases for larger look-ahead times is because of the assumption that the look-ahead sensor can essentially see through intervening terrains, resulting in increased impact probability for extended look-ahead times. In particular, the model for the forward-looking sensor, as described in this section, is limited, in that the sensor is capable of seeing only the terrain at the look-ahead interval rather than scanning the terrain in this interval. Thus, if the terrain at the look-ahead interval has a lower altitude than the intermediate terrain, the control system will follow the lower-altitude terrain and the missile will strike the intermediate terrain. A more realistic model would consider a control system which has memory regarding the maximum altitude in the look-ahead interval; however, such a model is difficult to evaluate by analytic means, but can be investigated via an extensive computer simulation. Such a simulation has recently been performed⁶ and resulted in command clearance altitude about 25% lower than that generated by the method of this section.

Conclusions

The bald terrain impact probability of a terrain-following missile with a linear altitude control system, having either a downward or a forward-looking sensor, has been determined with emphasis on a terrain whose power spectral density decays at 20 dB/dec. In this case, previously published methods could not be used. For a downward-looking altitude control system bandwidth of 1 rad/sec and a terrain break frequency of 10^{-4} r/m, a cruise missile can be flown (see Fig. 9) with a very low impact probability (0.01 for 1000 km flight) at a mean clearance altitude of about 0.8 terrain (detrended) standard deviations at subsonic speeds ($M \sim 0.7$) and 1.5 terrain (detrended) standard deviations at supersonic speeds ($M \sim 3$). For faster responding control systems, it is possible to reduce the mean clearance altitude, but with a considerable increase in acceleration variance and corresponding range loss. If one assumes an accurate forward-looking sensor with a range of about 0.35 km, the mean clearance altitude can be reduced by a factor of one-half in comparison with a downward-looking case for the same impact probability.

A significant probability exists for a cruise missile flying at very low altitudes with a downward-looking control system to impact obstacles for reasonable values of the mean distance between obstacles and of the reconnaissance and navigational errors. For example, from Fig. 4 for subsonic flight at an altitude of 15 m, the probability of impacting an obstacle is about 0.15 for a standard deviation of navigational and reconnaissance errors of 1 km, compared to a 0.01 probability of impacting the bare terrain which has a standard deviation of 15 m and otherwise meets the terrain and control conditions previously specified.

References

- ¹ Earshen, J.J., "Terrain Avoidance-Display Evaluation Simulator-Project RED TAVERN," Cornell Aeronautical Lab., Cornell Univ., Ithaca, N.Y., Rept. GM 776-T-66, AD112706, Sept. 1956.
- ² Pelton, F., "Advanced Concepts for Terrain Avoidance (AD-CON)," Cornell Aeronautical Lab., Cornell Univ. Ithaca, N.Y., Rept. 1H-1224-P-11; Aeronautical Systems Div., Rept. ASD61-468, Oct. 1961.
- ³ Cunningham, E.P., "Probability of Crashing for a Terrain-Following Missile," *Journal of Spacecraft and Rockets*, Vol. 11, April 1974, pp. 257-260.
- ⁴ Rice, S., "Mathematical Analysis of Random Noise," reprinted in *Selected Papers on Noise and Stochastic Processes*, Dover Publications, New York, 1954, pp. 189-195.
- ⁵ Papoulis, *Probability, Random Variables and Stochastic Processes*, McGraw Hill, New York, 1965, Ch. 14, pp. 485-491.
- ⁶ Kerchner, R., private communication, Nov. 21, 1974, General Research Corp., McLean, Va.